Hamburger Beiträge
zur Angewandten Mathematik

An asymptotic numerical analysis of Hopf periodic traveling waves for a microscopic traffic problems

Bodo Werner

Nr. 2011-12
June 2011

An asymptotic numerical analysis of Hopf periodic traveling waves for a microscopic traffic problems

Bodo Werner *

June 15, 2011

Abstract

We consider the simplest follow-the-leader microscopic traffic model with N cars on a circle of length L with an optimal velocity function V due to [BHN+95]. Besides of N and L, this model has three system parameters, a, τ and v_{max}, see (1). By several numerical experiments we study the dynamics of stable periodic solutions (periodic in headway and speed) which exist due to Hopf bifurcations (see [GSW04]).

Being interested in an asymptotic analysis for N (and L) large enough we discovered a surprising result: For given system parameters a, τ and v_{max} all periodic solutions have the same dynamical structure independent of L and N: Each car drives either slowly with small headway h_c and small speed v_c (congestive dynamics) or with large headway h_f and large speed v_f (non-congestive). Each part represents a stable quasi-stationary dynamics. The transient part where a car accelerates or decelerates is almost independent of N and is hence negligible. The basic parameters h_c and h_f determine the whole dynamics since all other quantities connected with a periodic solution can be analytically expressed through these two "magic" parameters.

Particularly the jam speed σ does not depend on L and N, the period T_N is proportional to N and does not depend on L, see Theorem 1 which is not proved, but confirmed by numerical computations.

The traveling wave character of the periodic solutions is obvious from the macroscopic visualizations with a straight line profile, see Fig. 2(b) (speed) and Fig. 2(c) (headway). This allows to compute "macroscopic" real functions v (speed) and h (headway) implicitly defined by

$$\dot{x}_j(t) =: v((x_j(t) - \sigma t) \bmod L), \quad x_{j+1}(t) - x_j(t) =: h((x_j(t) - \sigma t) \bmod L),\ j = 1, 2, ..., N.$$

They seem to have a universal structure, almost independent of N and L. They satisfy a differential-functional-system with delay depending on the state which may have a heteroclinic connection, see Sec. 4.

Keywords: Microscopic traffic model, numerical bifurcation analysis, Hopf bifurcation, periodic solutions, traveling waves

AMS subject classification: 37M20, 65L07, 65P30, 65P40

1 Introduction

We study the microscopic N-car traffic model on a circle of length L with identical drivers which was presented originally by Bando et al [BHN+95]

$$\ddot{x}_j(t) = \frac{1}{\tau}\Big(V(x_{j+1}(t) - x_j(t)) - \dot{x}_j(t)\Big), j = 1, ..., N, x_{N+1} = x_1 + L \tag{1}$$

with the optimal velocity function

$$V(y) = v_{max}\frac{\tanh a(y-1) + \tanh a}{1 + \tanh a}. \tag{2}$$

*Department of Mathematics, University of Hamburg, Bundesstr. 55, D-20146 Hamburg, Germany

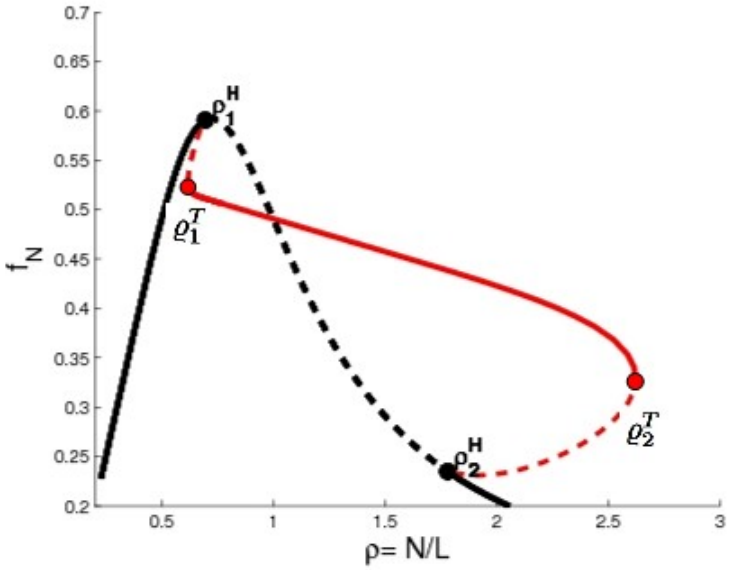

Figure 1: $N = 20, a = 2, v_{Max} = 1, \tau = 1$: Solution diagram for Hopf-periodic solutions

Various authors have studied this model and certain extensions (see [GSW04], [GW10], where bottlenecks are studied, and the references therein).
This paper is based on model (1) and investigates the periodic solutions due to Hopf bifurcations as studied by [GSW04].
There exist very simple *quasi-stationary solutions* given by

$$x_j^0(t) = j\frac{L}{N} + t\,V\Big(\frac{L}{N}\Big) + c, \qquad j = 1, ..., N. \tag{3}$$

with constant velocities $V(\frac{L}{N})$, constant headways $\frac{L}{N}$ and an arbitrary constant c.
It is well-known that they are asymptotically stable if

$$V'\Big(\frac{L}{N}\Big) < \frac{1}{1+\cos\frac{2\pi}{N}}$$

(see [Hui02, GSW04]). Critical parameter values where Hopf bifurcations with respect to the circle length L occur, are defined by $V'(\frac{L}{N}) = \frac{1}{1+\cos\frac{2\pi}{N}}$.

We will focus on the dependence of the bifurcating *Hopf-periodic solutions* on the traffic density $\varrho = \frac{N}{L}$ (instead on L). For fixed N, there exist two *Hopf densities* $\varrho_{N,1}^H < \varrho_{N,2}^H$ depending on the number N of cars. Fig. 1 shows a typical solution diagram, where we choose the average flow $f_N := \varrho v_N$ as characteristic number of the Hopf-periodic solutions (in red) and of the quasi-stationary solutions (in black) (v_N is the average speed).
The Hopf densities satisfy $V'(1/\varrho_{N,j}^H) = \frac{1}{1+\cos(2\pi/N)}$, $j = 1, 2$. For $N \to \infty$ they converge against the *asymptotic Hopf densities*[1] $\varrho_{\infty,1}^H < \varrho_{\infty,2}^H$ which satisfy $V'(1/\varrho_{\infty,j}^H) = \frac{1}{2}$, $j = 1, 2$. More important for our experiments are the two turning points (red dots in Fig. 1) on the red path of periodic solutions with densities $\varrho_j^T, j = 1, 2$ which satisfy[2]

$$\varrho_1^T < \varrho_1^H < \varrho_2^H < \varrho_2^T.$$

[1] For $a = 2, v_{max} = 1, \tau = 1$ we have $\varrho_{\infty,1}^H = 0.691 < \varrho_{\infty,2}^H = 1.809$
[2] For $a = 2, v_{max} = 1, \tau = 1$ and $N = 20$ we compute $\varrho_1^T = 0.618$ and $\varrho_2^T = 2.62$.

For all ϱ with $\varrho_1^T < \varrho < \varrho_2^T$ there is a unique stable periodic solution[3] – at least for the parameters in the caption of Fig. 1.

A typical (stable) periodic solution is a traveling wave with a dramatic jam as in Fig. 2 for $N = 40$ cars. Here Fig. 2(b) and 2(c) show macroscopic visualizations of speed and headway, while Fig. 2(a) shows the speed and the headway of a single car as function of time.

Since the isolines in Fig. 2(b) are straight lines with negative slope, one can conclude that the wave travels upstream[4] with constant speed. We call this speed the jam (congestion) speed σ which is negative for an upstream flow. The straight line property can easily been shown and a formula for σ, see (5) in Sec. 2, is obtained which involves the time period T of the Hopf-periodic solution being the time a single car travels between two jam events.

The most important quantities of Hopf-periodic solutions are the following ones (here c stands for **c**ongestion and f for (congestion-) **f**ree traffic):

1. N, L and the density $\varrho = \frac{N}{L}$
2. the reduced Hopf period $T^r := \frac{T}{N}$, where T is the Hopf period
3. the jam speed σ
4. the minimal headway h_c and the minimal speed v_c
5. the maximal headway h_f and the maximal speed v_f

Observe that these numbers depend on the specific periodic solution and hence on N and on the density $\varrho = \frac{N}{L}$ which has to satisfy $\varrho_1^T < \varrho < \varrho_2^T$ with the turning point densities $\varrho_j^T, j = 1, 2$ explained above. The periodic solutions are numerically determined by computing the fixed points of a symmetry reduced Poincaré map, similar as in [GW10] and [SGW09]. The jam speed σ is computed by formula (5).

The surprising result of our numerical experiments (see Sec. 3) is the following: All numbers above are *asymptotic* in the sense that their limits for $N \to \infty$ exist for fixed $\varrho = \frac{N}{L}$ and that the limits do not depend on ϱ. Moreover, the two limits for h_c and h_f (which we also call h_c and h_f) determine all other asymptotic limits and hence the whole dynamics. The limits can be analytically expressed by these two numbers which we therefore – following INGENUIN GASSER – call "magic":

$$v_c = V(h_c),\ v_f = V(h_f),\ \sigma = \frac{h_c v_f - h_f v_c}{h_c - h_f},\ T^r = \frac{h_f - h_c}{v_f - v_c},$$

see Sec. 2. These relations can be easily verified from numerical results. Hence, for sufficiently large N and for all densities ϱ (and for all circle lengths L) the numbers above are well approximated by their asymptotic limits as long as the density ϱ allows the existence of a stable periodic solution ($\varrho_1^T < \varrho < \varrho_2^T$). Roughly speaking, all numbers do not depend on N and on L.

Moreover, the numerical results state that the Hopf periodic solutions essentially consist of three parts: The congestive part with small identical headways h_c and small speeds v_c, the non-congestive part with large identical headways h_f and large speeds v_f and some transient parts which seem to have a size independent of N and hence negligible for large N, see Fig. 9. The first two parts correspond to two stable quasi-stationary solutions with headways h_c and h_f. The corresponding densities $\varrho_c := \frac{1}{h_c}$ and $\varrho_f := \frac{1}{h_f}$ can be located in those parts of the solution diagram (as Fig. 1) where no stable periodic solutions exist. We guess that ϱ_c and ϱ_f are the limits of the turning point densities $\varrho_j^T, j = 1, 2$ above for $N \to \infty$, see Sec. 3.5. Two Hopf-periodic solutions only differ in the width L_c of the congestive and the width L_f of the non-congestive parts. If ϱ is small (large), so also the congestive part, see the asymptotic formula (8) in Theorem 1.

[3] The Hopf bifurcations seem to be obviously subcritical in contradiction to the supercriticality statement in [GSW04]. A more thorough computation shows that the supercriticality is an almost unvisible phenomenon, it takes place only in a very small neighborhood of the Hopf bifurcation points.

[4] against the traffic direction

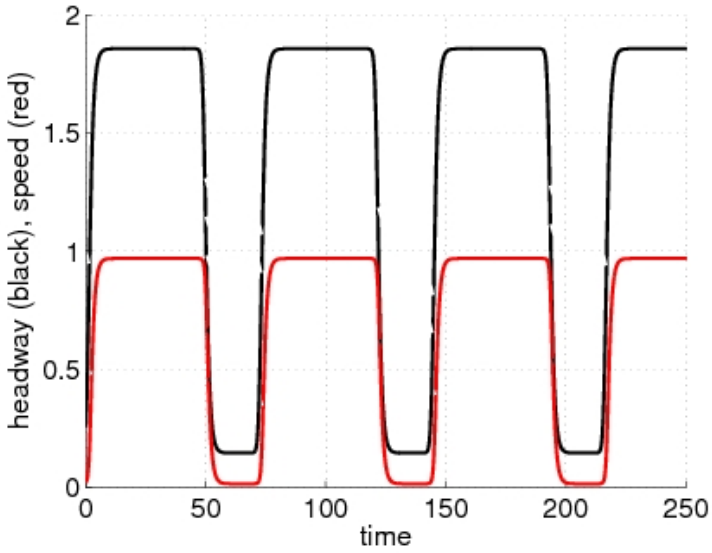

(a) Time-headway-speed functions

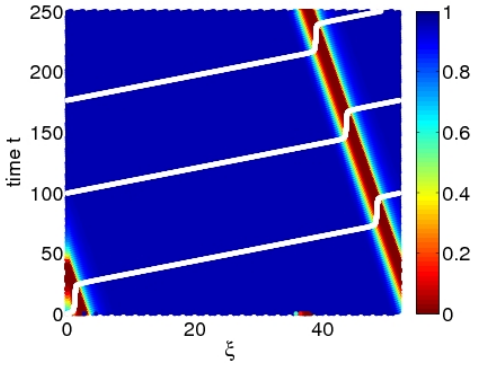

(b) Macroscopic visualization (color=speed)

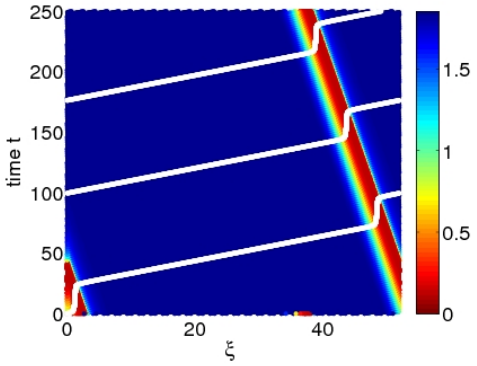

(c) Macroscopic visualization (color=headway)

Figure 2: $N = 40, \varrho = 0.769\,(L = 52), a = 2, v_{max} = 1, \tau = 1$: Stable periodic solution

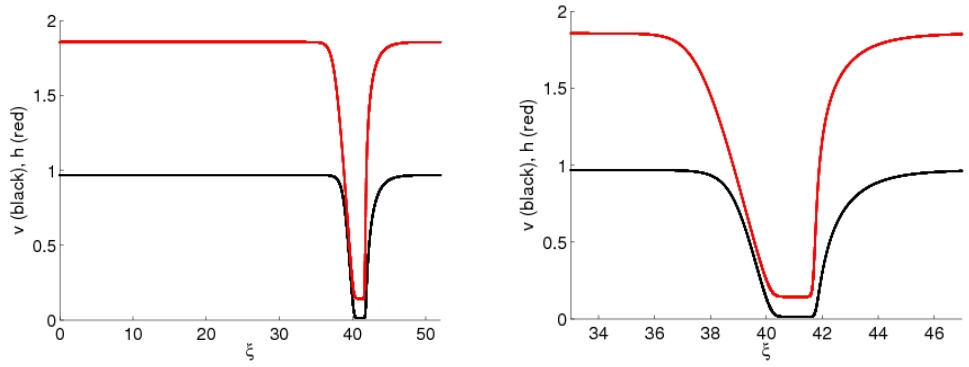

(a) headway-speed function (b) Detail of Fig. 3(a)

Figure 3: $N = 40$, $\varrho = 0.769$ $(L = 52)$, $a = 2$, $v_{max} = 1$, $\tau = 1$: Macroscopic speed- and headway functions v and h

From the straight line structure in the macroscopic view of speed (Fig. 2(b)) and of headway (Fig. 2(c)) we conclude that there are *macroscopic*[5] real functions $v(\xi)$ (speed) and $h(\xi)$ (headway) of space ξ which are L-periodic and implicitly defined by

$$\dot{x}_j(t) =: v((x_j(t) - \sigma t) \bmod L), \quad x_{j+1}(t) - x_j(t) =: h((x_j(t) - \sigma t) \bmod L),\ j = 1, 2, ..., N.$$

They can be computed as a by-product from the trajectories of the Hopf periodic solution (Sec. 3.4), see Fig. 3 for an example. They seem to be smooth and to describe the whole dynamics in a transparent way.

It turns out that all such macroscopic functions have essentially the same shape, they only differ in the widths of the valleys and of the mountains, not in the width of the transient parts. They can be obtained by a traveling wave Ansatz for the infinite follow-the-leader-problem on an infinite line. The resulting equation is a complicated ODE-system with delay depending on the state which may have a heteroclinic connection, see Sec. 4.

As a consequence we claim that our traveling wave solutions somehow survive on the infinite line ($L \to \infty$) if the average density ϱ satisfies $\varrho_f < \varrho = \frac{N}{L} < \varrho_c$.

2 Some theory

Having identical cars, the Hopf-periodic solutions with period T_N satisfy

$$v_j(t + T_N/N) = v_{j+1}(t)$$

for the speed $v_j(t)$ of car No. j at time t. An analogue relation holds for the headways $h_j(t)$, see [SGW09].

The statement that the speed isolines are straight can be formulated by the fact that the numbers

$$s_N := x_j(t + T_N/N) - x_{j+1}(t) \tag{4}$$

are independent of j and t. This can be easily been shown and we obtain[6] the formula

$$\sigma_N = \frac{N \cdot s_N}{T_N} \tag{5}$$

[5] We choose this name because this type of functions would be encountered by a traveling wave solution of a PDE.
[6] Determine the slope of the isolines in Fig. 2(b).

for the jam speed σ_N. Our numerical computation of σ_N in Sec. 3 is based on (5). Hence the jam travels upstream for negative values of s_N. Numerical results show that T_N/N and σ_N are asymptotic.
Observe that T_N is the time a single car spends between two jam events like entering or leaving the jam area.

For the following relations we assume that the observations, described in the introduction and confirmed by numerical experiments in Sec. 3, hold. More precisely, we assume — neglecting the transition between congestion and non-congestion — that each car either drives with minimal speed v_c or with maximal speed v_f, that headways are either minimal (h_c) (c=congestion) or maximal (h_f (f=free)). Then

$$\varrho_c := \frac{1}{h_c},\ \varrho_f := \frac{1}{h_f}$$

can be interpreted as traffic densities in the jam area and non-jam area respectively.
For simplicity, we replace the index f by 1 and c by 2. Then $h_1 = h_f > h_2 = h_c, v_1 = v_f > v_2 = v_c, \varrho_1 = \varrho_f < \varrho_2 = \varrho_c$. For fixed time, the whole circle of length L consists of a non-jam part with length $L_1 := L\frac{\varrho_2-\varrho}{\varrho_2-\varrho_1}$ and of a jam part of length $L_2 := L\frac{\varrho-\varrho_1}{\varrho_2-\varrho_1}$. Using a coordinate system which rotates with speed σ, the cars have the speeds $v_1 - \sigma$ or $v_2 - \sigma$. Obviously the time a car passes through the headway in these coordinates, is independent of the position and equals $T^r = \frac{T}{N}$. Hence

$$\frac{h_1}{v_1-\sigma} = \frac{h_2}{v_2-\sigma} = \frac{T}{N} = T^r. \tag{6}$$

(6) is equivalent to

$$\varrho_1(v_1-\sigma) = \varrho_2(v_2-\sigma) = \frac{1}{T^r}$$

which is nothing else than the invariance of the relative flow, relative with respect to an observer who is sitting on the wave.
By elementary calculations, we get the formulas

$$\sigma = \frac{h_1v_2 - h_2v_1}{h_1 - h_2}$$

for the jam speed[7] and

$$T^r := \frac{T}{N} = \frac{h_1 - h_2}{v_1 - v_2}$$

for the reduced period.
For the times T_1 resp. T_2, a car needs to pass through the non-jam- resp. the jam area we have the simple expressions

$$\frac{T_1}{N} = \frac{h - h_2}{h_1 - h_2},\quad \frac{T_2}{N} = \frac{h_1 - h}{h_1 - h_2}$$

with $h := \frac{L}{N}$.

Our numerical results let us state the following

Theorem 1. *Consider the ODE system (1) modeling the dynamics on N cars on a circle of length L with the optimal velocity function (2) and system parameters τ, a, v_{max}. We assume that the solution diagram is like that in Fig. 1 with Hopf densities ϱ_j^H and turning point densities $\varrho_j^T, j = 1, 2$ satisfying*

$$\varrho_1^T < \varrho_1^H < \varrho_2^H < \varrho_2^T.$$

[7] Thanks to Ingenuin Gasser

We further assume that the global density $\varrho := \frac{N}{L}$ satisfies $\varrho_1^T < \varrho < \varrho_2^T$ such that there is a unique stable periodic solution. Let h_c, h_f, v_c, v_f, T^r and σ be the characterizing quantities of the periodic solution as described above [8]. Define the densities[9] $\varrho_c := \frac{1}{h_c}, \varrho_f = \frac{1}{h_f}$.
Then – for large enough N – the two "magic" headways h_c and h_f do not depend on N and determine all other quantities by

$$\begin{aligned} v_c = V(h_c),\ v_f = V(h_f), \\ \sigma = \frac{h_c v_f - h_f v_c}{h_c - h_f}, \\ T^r = \frac{h_f - h_c}{v_f - v_c}. \end{aligned} \tag{7}$$

Moreover,

- *The period T_N of the periodic solution does not depend on L and satisfies $T_N = N \cdot T^r$.*
- *For fixed time t, the car ensemble on the circle essentially consists of two parts, the congestive and the non-congestive part. The congestive part contains cars with headways h_c and speeds v_c and the non-congestive part contains cars with headways h_f and speeds v_f. The length L_c (resp. L_f) of the congestive (resp. non-congestive) part satisfies*

$$L_c = L\frac{\varrho - \varrho_f}{\varrho_c - \varrho_f}, \quad L_f = L - L_c. \tag{8}$$

- *The smaller $\varrho - \varrho_f$ the smaller is the relative length L_c/L of the congestive part. The smaller $\varrho_c - \varrho$ the smaller is the relative length L_f/L of the non-congestive part.*
- *The congestive part (the jam) (and also the non-congestive part) moves upstream (against the traffic direction) with speed σ.*
- *The limit densities ϱ_c and ϱ_f are the limits of turning point parameters $\varrho_j^T, j = 1, 2$ for the solution diagram of periodic solutions for fixed N when N tends to infinity.*
- *The infinite microscopic ODE-system possesses a traveling wave with speed σ connecting a congestive flow (with speed v_c and density ϱ_c) with a non-congestive flow (with speed v_f and density ϱ_f). The traveling wave can be associated with a heteroclinic orbit of an ODE-delay equation.*

For $a = 2, v_{max} = 1, \tau = 1$ in the microscopic Bando traffic model we obtain the numerical values (see next Section)

$$h_c = 0.1441,\ h_f = 1.8559,\ \varrho_c = 6.9396,\ \varrho_f = 0.5388,$$

$$v_c = 0.013829,\ v_f = 0.96786,\ \sigma = -0.066485,\ T^r = 1.79428.$$

For values for other parameters see Sec. 3.6.

3 Numerical results

3.1 Asymptotic numbers

We choose $a = 2, v_{max} = 1, \tau = 1$ as in [GW10]. Table 1 contains the most important numbers of a periodic solution for different values of N and L (resp. ϱ) like jam speed σ, the minimal and maximal headways h_c and h_f (resp. speeds v_c and v_f) and the reduced period $T^r := T/N$. There is no doubt about their asymptotic property, stated in Theorem 1,

[8] They can be easily computed once the periodic solutions is determined.
[9] of the corresponding quasi-stationary solutions

independent of the way how $L, N \to \infty$. The results for $N = 100, \varrho = 0.571$ (fifth row) are less significant since the density $\varrho = 0.571$ is close to the turning point density $\varrho_1^T = 0.559$. The maximal absolute value of Floquet multipliers which are not shown varies between 0.92 and 0.99.
The formulas in Theorem 1 can easily been checked.

Table 1: Jam speed, minimal and maximal headways and speeds, reduced period

N	L	ϱ	σ	h_c	v_c	h_f	v_f	$T^r = T/N$
20	26	0.769	-0.066495	0.146	0.01465	1.85584	0.96785	1.794221
40	60	0.667	-0.664852	0.1443374	0.01393	1.855892	0.96785	1.794279
40	50	0.800	-0.0664848	0.1441059	0.013829	1.855894	0.96786	1.794276
80	40	2.000	-0.0664846	0.1441050	0.013829	1.855897	0.96786	1.794280
100	175	0.571	-0.0665018	0.1468262	0.015002	1.855807	0.96784	1.794184
100	164	0.609	-0.0664847	0.1441072	0.01383	1.855894	0.96786	1.794279
100	150	0.667	-0.0664842	0.1441047	0.013829	1.855897	0.96786	1.794282
100	100	1.000	-0.0664847	0.1441053	0.013829	1.855895	0.96786	1.794279
100	70	1.429	-0.0664847	0.1441056	0.013829	1.855894	0.96786	1.794279
100	50	2.000	-0.0664845	0.1441033	0.013829	1.855896	0.96786	1.794280
100	30	3.333	-0.0664851	0.1441063	0.013829	1.855802	0.96781	1.794278
150	150	1.000	-0.0664847	0.1441039	0.013829	1.855896	0.96786	1.794279
200	280	0.7143	-0.0664846	0.1441054	0.013829	1.855895	0.96786	1.794280
200	200	1.000	-0.0664847	0.1441040	0.013829	1.855896	0.96786	1.794279
300	400	0.750	-0.0664852	0.1441057	0.013829	1.855894	0.96786	1.794277
300	100	3.000	-0.0664843	0.1441049	0.013829	1.855897	0.96786	1.794281

In the following subsections we visualize the Hopf-periodic traveling waves in three different ways as shown in Fig. 4 and Fig. 5. More precisely, we visualize the dynamics of the speed v and the headway h first as functions of time, second by a macroscopic view where the color is chosen according to the size of speed (choosing headway we would get qualitatively the same result) and third as macroscopic functions of space and third .

3.2 Speed and headway as function of time

Fig. 6 shows for $N = 100$ and various densities ϱ the speed v and the headway h as functions of time t from one period interval $[0, T]$. The results confirm our observations stated in Theorem 1. Observe that the jam area is very small for low densities, but becomes for high densities as large as the non-jam area for low densities.

3.3 Macroscopic view of the speed

[GW10] contains many colorful views, not only of traveling waves, but more frequently of quasi-POMs arising in case of bottlenecks instead of periodic solutions.
The introduction (Fig. 2(b) and Fig. 2(c)) contains an example of the macroscopic views of speed and headway). Other examples are given in Fig. 4(b) and Fig. 5(b).
Here, in Fig. 7, we are showing the evolution of such speed views for fixed $N = 100$ by varying ϱ, starting with small ϱ where the congestion width L_c is very small, and finally with large density ϱ, where now the jam width L_c almost equals L.

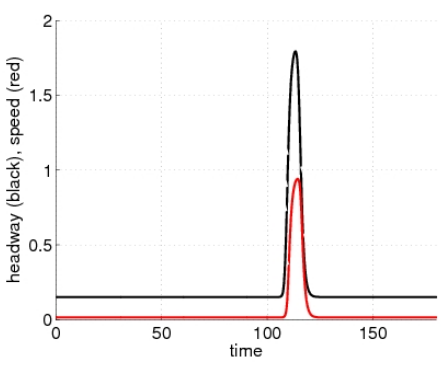

(a) Headway and speed as functions of time

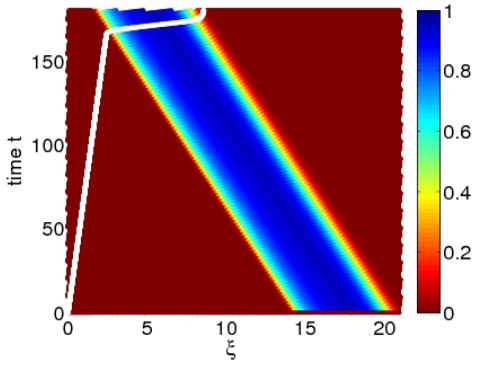

(b) Macroscopic visualization (color=speed)

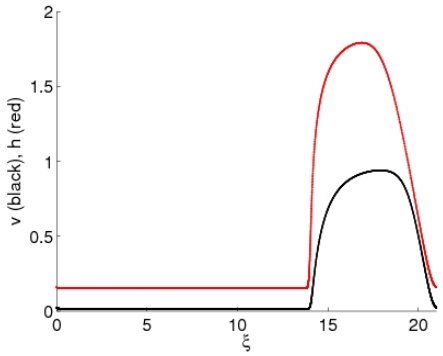

(c) Macroscopic headway and speed as functions of space

Figure 4: $N = 100, L = 21$ ($\varrho = 4.762$): Periodic solution in different representations

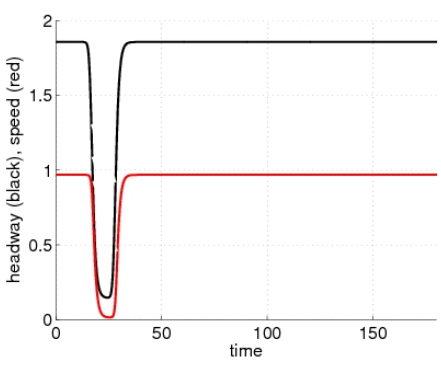

(a) Headway and speed as functions of time

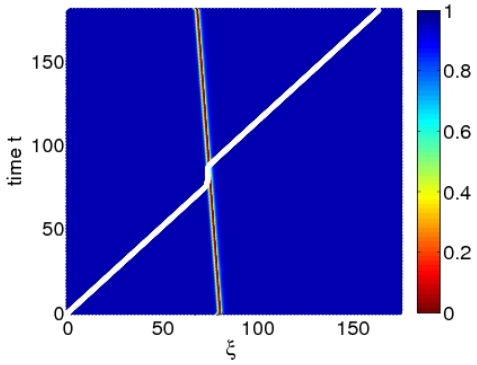

(b) Macroscopic visualization (color=speed)

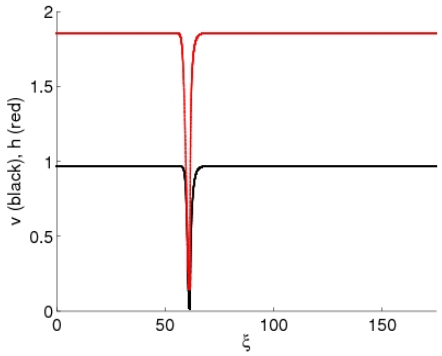

(c) Macroscopic headway and speed as functions of space

Figure 5: $N = 100, L = 75\,(\varrho = 1.3333)$: Periodic solution in different representations

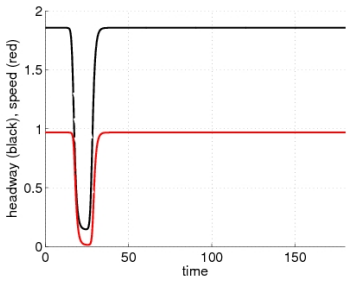

(a) $\varrho = 0.571\,(L = 175)$

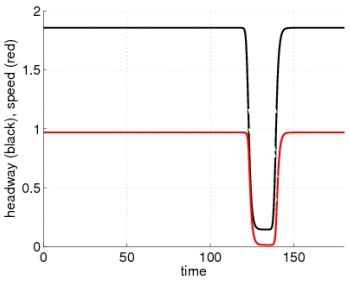

(b) $\varrho = 0.588\,(L = 170)$

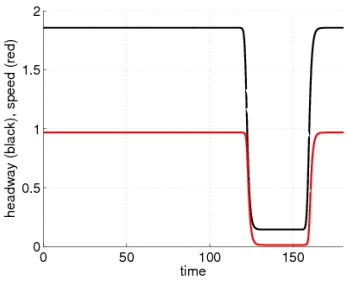

(c) $\varrho = 0.667\,(L = 150)$

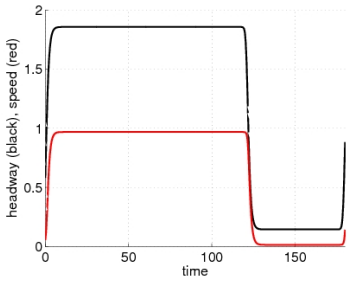

(d) $\varrho = 0.769\,(L = 130)$

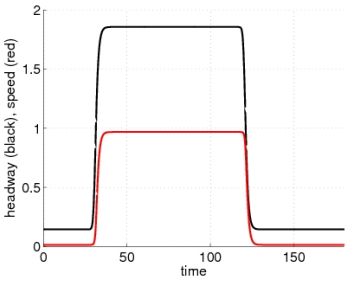

(e) $\varrho = 1.000\,(L = 100)$

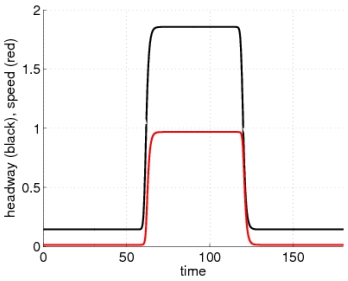

(f) $\varrho = 1.429\,(L = 70)$

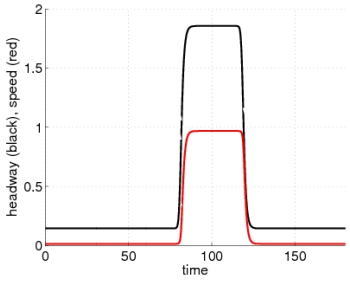

(g) $\varrho = 2.000\,(L = 50)$

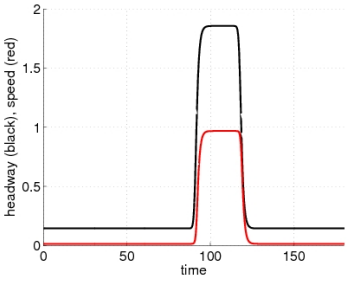

(h) $\varrho = 2.500\,(L = 40)$

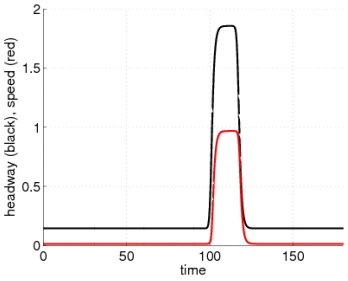

(i) $\varrho = 3.333\,(L = 30)$

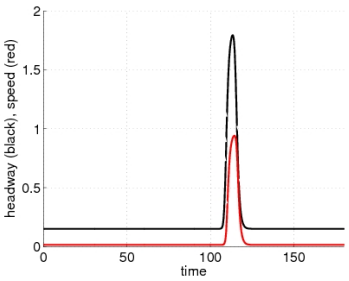

(j) $\varrho = 4.762\,(L = 21)$

Figure 6: $N = 100$: Headway h (red) and speed v (black) as function of time

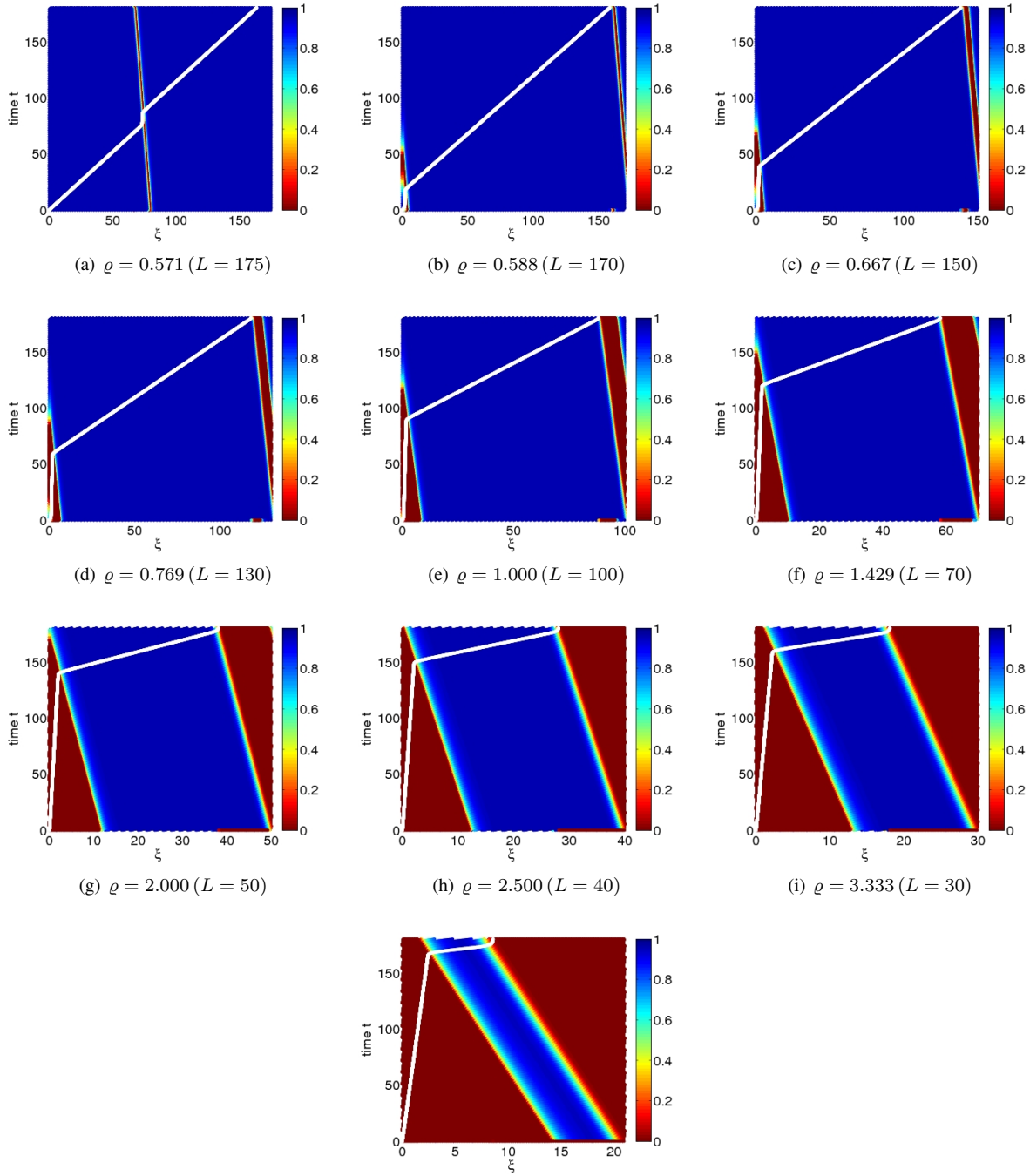

(a) $\varrho = 0.571\,(L = 175)$ (b) $\varrho = 0.588\,(L = 170)$ (c) $\varrho = 0.667\,(L = 150)$

(d) $\varrho = 0.769\,(L = 130)$ (e) $\varrho = 1.000\,(L = 100)$ (f) $\varrho = 1.429\,(L = 70)$

(g) $\varrho = 2.000\,(L = 50)$ (h) $\varrho = 2.500\,(L = 40)$ (i) $\varrho = 3.333\,(L = 30)$

(j) $\varrho = 4.762\,(L = 21)$

Figure 7: $N = 100$: Macroscopic visualizations of speed with increasing density)

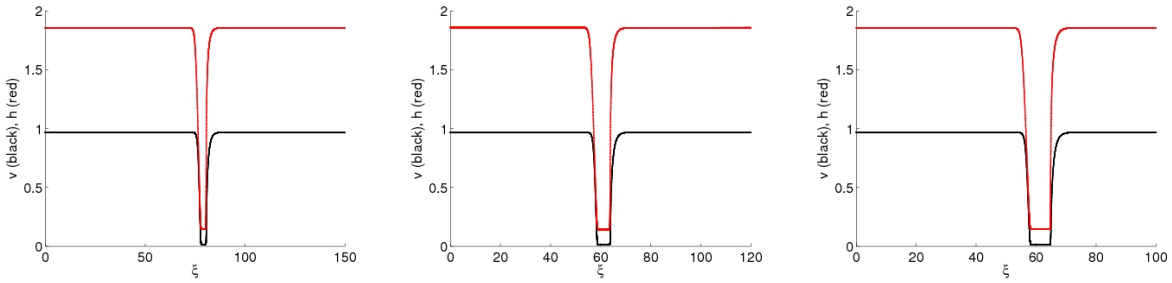

(a) $\varrho = 0.6667\,(L = 150)$) (b) $\varrho = 0.8333\,(L = 120)$ (c) $\varrho = 1.0000\,(L = 100)$

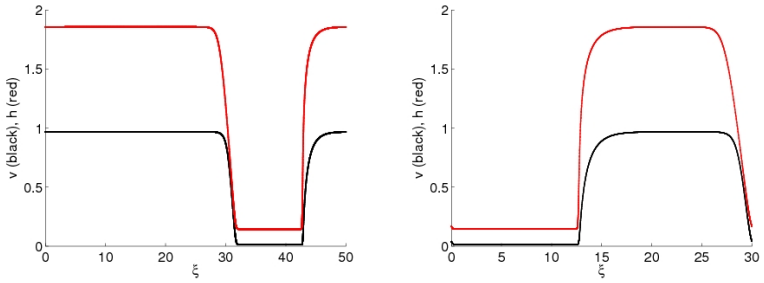

(d) $\varrho = 2.0000\,(L = 50)$ (e) $\varrho = 3.3333\,(L = 30)$

Figure 8: $N = 100$: Macroscopic headway (red) and speed (black) functions

3.4 Macroscopic functions

In the introduction we introduced the important concept of macroscopic functions of space — the speed $v(\xi)$ and the headway $h(\xi)$. Observe that for each time t for which we compute $x_j(t), \dot{x}_j(t), j = 1, 2, ..., N$ we obtain N points of the graphs of v and of h by the implicit setting

$$\dot{x}_j(t) = v((x_j(t) - \sigma t) \bmod L), \quad x_{j+1}(t) - x_j(t) = h((x_j(t) - \sigma t) \bmod L),\ j = 1, 2, ..., N.$$

If we simulate the ODE system for a while we will get sufficiently many points of the graphs to draw a "continuous" picture. Fig. 3 shows some introductory example. Fig. 8 shows further pictures for $N = 100$ and various densities ϱ. It becomes obvious that the width of the jam area increases with increasing density ϱ. Moreover, the functions seem to be smooth, at least continuous.

When we investigate the transition area of our macroscopic functions we encounter the same shape for all sufficiently large N. This is confirmed by Fig. 9.

To find out how many cars stay in the transition area at a fixed time, Fig. 10 tells us that the (small) number (about 3-5 cars) does asymptotically not depend on ϱ.

From these calculations we may draw the following somehow speculative conclusion: For large enough N and L we obtain smooth L-periodic macroscopic functions v and h which are composed by four parts, the congestive part v_-, the non-congestive part v_+ and the two transient parts $v_{-,+}$ (from v_- to v_+) and $v_{+,-}$ (from v_+ to v_-). They only differ by variation of L and N in the widths of the (non-)congestive parts.

In Sec. 4 some possible analytical background is discussed.

3.5 Turning points

If our statement about the turning point densities $\varrho_j^T, j = 12$, is right, an upper (lower) bound for the lengths L where periodic solutions exist are $N \cdot h_f$ and $N \cdot h_c$. The corresponding densities are $\varrho_c = 6.9396$ and $\varrho_f = 0.53028$. Our

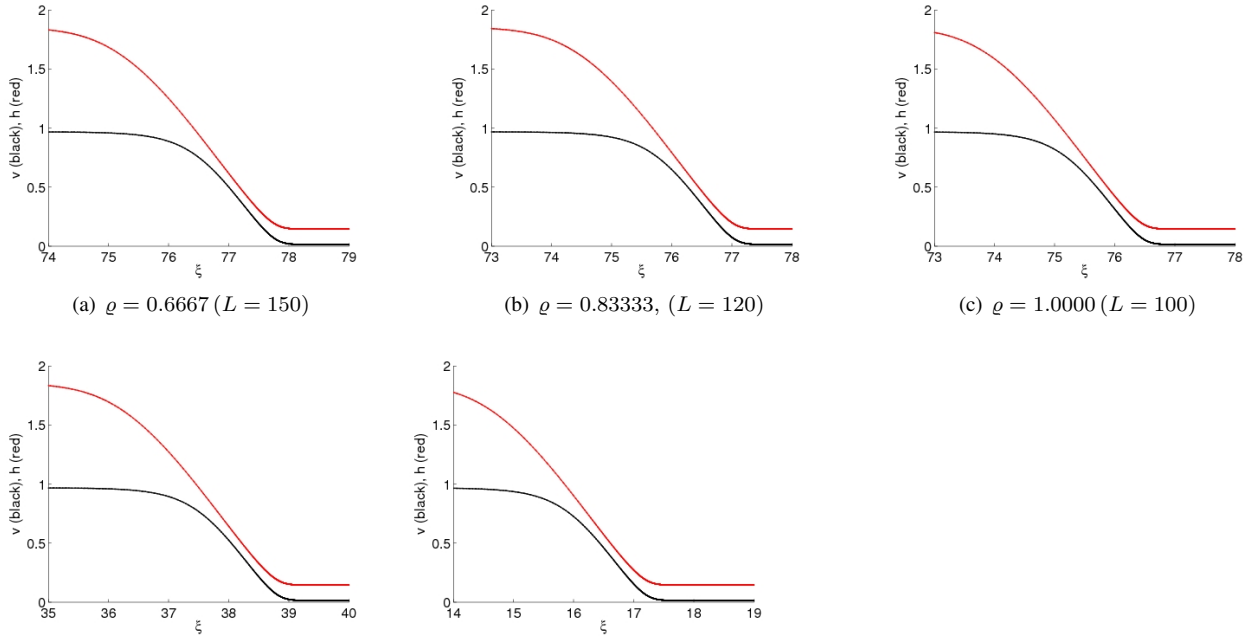

(a) $\varrho = 0.6667\,(L = 150)$ (b) $\varrho = 0.83333,\ (L = 120)$ (c) $\varrho = 1.0000\,(L = 100)$

(d) $\varrho = 2.0000\,(L = 50)$ (e) $\varrho = 3.3333\,(L = 30)$

Figure 9: $N = 100$: Transition of macroscopic headway ($h_{+,-}$) and speed functions ($v_{+,-}$) from non-congestive to congestive flow

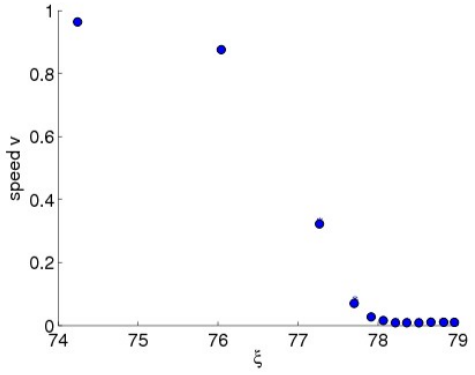

(a) $L = 150 : v_{+,-}$

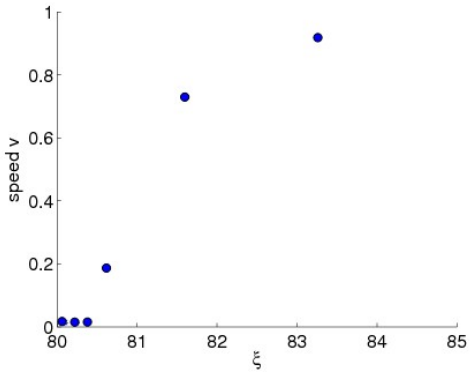

(b) $L = 150 : v_{-,+}$

]

(c) $L = 100 : v_{+,-}$

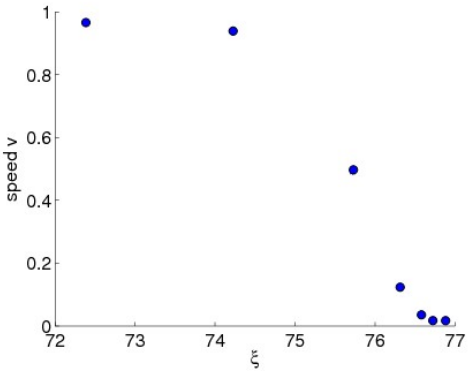

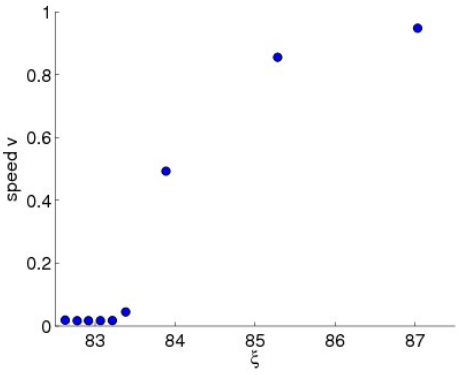

(d) $L = 100 : v_{-,+}$

]

(e) $L = 40 : v_{+,-}$

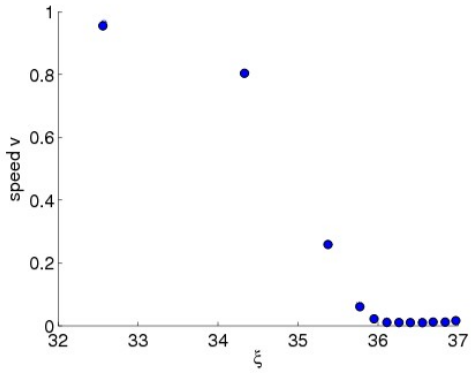

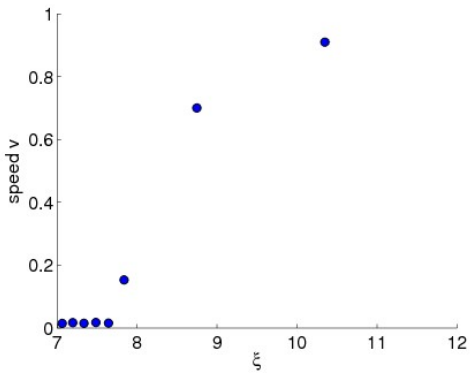

(f) $L = 40 : v_{-,+}$

Figure 10: $N = 100$: Distribution of cars at a fixed time in the transition between congestive and non-congestive area

conjecture is that they are the limits of turning point densities $\varrho_j^T, j = 1, 2$ in our solution diagram[10] for $N \to \infty$. Therefore we have computed the two turning points densities $\varrho_1^T < \varrho_2^T$ for different N which is very time consuming for large N:

Table 2: Turning point densities

N	ϱ_1^T	ϱ_2^T
20	0.618	2.62
40	0.582	3.545
100	0.559	4.783
200	0.555	5.546
400	0.549	5.964
800		> 6.4

Our conjecture is based on the fact that the limit of periodic solutions for small (large) ϱ is the quasi-stationary solution with headway h_f (h_c). The convergence $\varrho_1^T \to \varrho_f$ and $\varrho_2^T \to \varrho_c$ for $N \to \infty$ must be slow since the periodic solutions at the turning points have still a very small jam or non-jam area. They are still rather far away from the corresponding quasi-stationary solutions.

3.6 Remarks

The periodic solutions in the Bando-Model are not necessarely "physical" solutions with positive headways. This was the starting point in [BJ08] where a special kind of overtaking is allowed. They choose the same model as in this section, only $v_{max} = 7$ is chosen much higher.
Now it turns out that the positivity of the "magic" headway h_c seems to guarantee that all periodic solutions are physical. It might be interesting to investigate the dependence of h_c on the Bando parameters v_{max} and a, see Table 3. It is remarkable that the universal character of the headway h_c is also true for non-physical solutions (row 3). The loss of physicality of periodic solutions is accompanied by a decrease of the jam speed σ. Indeed: our analytical relation (7),

$$\sigma = \frac{h_c v_f - h_f v_c}{h_c - h_f},$$

verifies this fact. Physicality of periodic solutions are characterized by an upstream jam!

Table 3:

v_{max}	a	h_c	h_f	σ	T^r
1	2	0.1441	1.8559	-0.0665	1.794
1.1	2	0.0511	1.9489	-0.0244	1.772
1.2	2	-0.0380	2.038	0.0186	1.753
1	2.2	0.1428	1.8572	-0.0700	1.773
1	1.8	0.1496	1.8500	-0.0637	1.818
0.8	2	0.3502	1.6498	-0.1474	1.852

The decrease of v_{max} (last row) changes the quality of the periodic solutions. The minimal headway h_c is rather large, the maximal speed is rather far away from v_{max}.

[10] see Fig. 1 for $N = 20$. For larger N the red path of periodic solutions will expand to the left and to the right.

4 Differential-functional equation

Each periodic solution $x_j(t), j = 1, 2, ..., N$, of our model (1) is associated with *macroscopic real L-periodic functions* v and h, see Sec. 3.4. They are implicitly defined by

$$\dot{x}_j(t) =: v((x_j(t) - \sigma t) \bmod L), \quad x_{j+1}(t) - x_j(t) =: h((x_j(t) - \sigma t) \bmod L),\ j = 1, 2, ..., N. \tag{9}$$

Assuming differentiability, they fulfill[11] the system

$$v'(\xi)(v(\xi) - \sigma) = V(h(\xi)) - v(\xi), \tag{10}$$
$$h'(\xi)(v(\xi) - \sigma) = v(\xi + h(\xi)) - v(\xi). \tag{11}$$

The first equation is an ODE, the second equation is a functional-differential equation with ξ-depending anti-delay. Observe that this system does not depend on N and not on L. It can also be obtained by considering infinite many cars distributed somehow on the whole real line, where the dynamics is given by the infinite ODE system

$$\dot{h}_j(t) = v_{j+1}(t) - v_j(t),$$
$$\dot{v}_j(t) = \frac{1}{\tau}\Big(V(h_j(t)) - v_j(t)\Big),\ j \in \mathbb{Z}.$$

The condition at time $t = 0$ defines the initial distribution (headways) of cars and their speeds. Looking for traveling wave functions v and h for this infinite system we encounter the differential-delay system (10, 11) which seems to have a large family of (L-periodic) solutions.
We believe that there is also a very special "heteroclinic" solution. Resuming the discussion in Sec. 3.4 we compose a solution (v, h) by an infinite piece (v_+, h_+), the transient piece $(v_{+,-}, h_{+,-})$ and again an infinite piece (v_-, h_-), such that

$$v(\xi) \to v_f,\ h(\xi) \to h_f \text{ for } \xi \to -\infty,$$
$$v(\xi) \to v_c,\ h(\xi) \to h_c \text{ for } \xi \to +\infty.$$

holds.

Somehow our headways h_c and h_f seem to be hidden in the system (10, 11).

5 Conclusion

Many numerical calculations combined with some analysis let us conjecture that the stable periodic solutions of the simplest microscopic follow-the-leader-model have a very simple structure which can easily described by two numbers only, the headways h_c and h_f which depend on the system parameters τ, a and v_{max}. All other numbers like jam speed, period, jam length, etc can be analytically expressed by these quantities.
We introduce the concept of macroscopic real functions v (speed) and h (headway) which seem to have a universal structure and describe the dynamics for arbitrary (large) N (and L). Since there is still the hope that there is a macroscopic PDE model for speed and headway which possesses similar traveling waves, our macroscopic functions offer the opportunity for a quantitative comparison with the microscopic model.

References

[BHN+95] M. Bando, K. Hasebe, A. Nakayama, A. Shibata, and Y. Sugiyama. Dynamical model of traffic congestion and numerical simulation. *Phys. Rev. E*, 51:1035ff, 1995.

[11] Differentiation of (9) and use of the ODE system (1)

[BJ08] L. Buřič and V. Janovský. On pattern formation in a class of traffic models. *Physica D 237*, pages 28–49, 2008.

[GSW04] I. Gasser, G. Sirito, and B. Werner. Bifurcation analysis of a class of 'car following' traffic models. *Physica D*, 197/3-4:222–241, 2004.

[GW10] I. Gasser and B. Werner. Dynamical phenomena induced by bottlenecks. *Phil. Trans. R. Soc. A 368, 4543-4562*, 2010.

[Hui02] H. J. C. Huijberts. Improved stability bound for steady state flow in a car-following model of road traffic in a circular road. *Phys.Rev. E*, 65:?–?, 2002.

[SGW09] T. Seidel, I. Gasser, and B. Werner. Microscopic car-following models revisited: from road works to fundamental diagrams. *SIAM J. Appl. Dyn. Sys.*, 8 (3):1305–1323, 2009.